

# PHYSICAL REVIEW B

## SOLID STATE

THIRD SERIES, VOL. 2, No. 7

1 OCTOBER 1970

### Energy Levels of Uranium Ions in Calcium Fluoride Crystals

W. A. Hargreaves

*Optovac, Incorporated, North Brookfield, Massachusetts 01535*

(Received 1 June 1970)

The crystal-field-split levels of divalent, trivalent, and tetravalent uranium ions have been studied at 20°K in selected crystals having single charge-compensation sites. Complete calculations have been made for the free-ion energy levels of  $U^{4+}$ , with the pertinent constants determined as  $F_0=13\,175$ ,  $F_2=200$ ,  $F_4=40$ ,  $F_6=8.05$ ,  $\zeta_{5f}=1660$ , and  $\alpha=26$ . Also calculated crystal-field-split levels of  $U^{4+}$  in  $C_{3v}$  symmetry are compared to experimental values, and the various "best fit" values of the crystal-field constants determined. ESR results on trigonal  $CaF_2:U^{4+}$  are correlated with predicted values derived from optical measurements. Experimental studies of the  $U^{2+}$  ion in calcium fluoride are related to the probable  $U^{2+}$  configuration,  $f^3s$ . Crystal-field splittings of the lower levels of  $CaF_2:U^{2+}$  are determined from measurements of absorption and fluorescence at 20°K. The calculated value of  $\zeta_{5f}$  for  $U^{2+}$ , based on approximate  $L-S$  coupling conditions for the lowest levels, is  $1560\text{ cm}^{-1}$ , and is compared with a similarly calculated value for  $U^{3+}$  of  $1520\text{ cm}^{-1}$ . Experimental crystal-field-split levels of tetragonal  $CaF_2:U^{3+}$  are shown to fit symmetry requirements, and various laser wavelengths of  $CaF_2:U^{3+}$  are related to the level system derived from absorption and fluorescence measurements. Temperature shifts of crystal-field-split levels of uranium ions are also reported.

#### INTRODUCTION

A previous paper<sup>1</sup> presented various aspects of identification and of absorption and fluorescence characteristics of divalent, trivalent, and tetravalent uranium ions in fluoride crystals. Also, some related papers have been published involving ESR studies of these ions.<sup>2-6</sup>

Further work is reported in the present paper concerning crystal-field-splitting analyses of uranium ions in specific crystal-field sites in calcium-fluoride single crystals. Improved spectroscopic facilities have permitted a more adequate presentation of uranium ion energy-level systems than those of the previous paper.

The carefully selected crystal systems covered by this report involve uranium ions of three different valences in essentially single charge-compensation sites. Growth was performed under high vacuum conditions, which permitted the elimination of all oxygen and water contaminations, and in the presence of an adequate supply of  $F^-$  ions, allowing elimination of residual oxygen and the estab-

lishment of  $F^-$  (not  $O^{2-}$ ) compensation sites. Under these conditions the  $CaF_2:U^{2+}$  crystal has a characteristic apple-green color, the  $CaF_2:U^{3+}$  a ruby-red color, and the  $CaF_2:U^{4+}$  a yellow color. Various other colors which have been observed, such as cerise and shades of brown, involve mixed valence systems or crystals with oxygen contamination. The yellow  $CaF_2:U^{4+}$  can be readily reduced at room temperature with strong ultraviolet light, gradually converting to a brownish mixture of  $U^{3+}$  and  $U^{4+}$ , then to a violet-red crystal of strong  $U^{3+}$  content, and finally to a greenish  $CaF_2:U^{2+}$  crystal. This conversion can be monitored by the decrease in absorption in certain sharp infrared absorptions characteristic of  $U^{4+}$ , but the reduced ions so produced do not show sharp  $f$  to  $f$  transitions in the infrared region, apparently as a result of selection rule prohibitions. Complete reconversion of the irradiated crystal is effected by a short heating at  $100^\circ\text{C}$ .

The properties of  $CaF_2:U^{3+}$ , if such a crystal can exist, are unknown. Hexavalent uranium in  $CaF_2$  as a uranyl ion has been prepared in many

laboratories, including ours. The crystal is colorless, has no free  $f$  electrons, and shows strong green uranyl fluorescence to the ground state.

The main components of the instrumentation were a vacuum-type grating spectrometer,<sup>7</sup> a lock-in electronic amplifier,<sup>8</sup> and a vacuum cryostat,<sup>9</sup> which allowed measurements of absorption and fluorescence at crystal temperatures from 20 to 293 °K.

#### TETRAVALENT URANIUM IONS IN CaF<sub>2</sub>

Spectroscopic studies in the infrared, visible, and ultraviolet regions have revealed the crystal-field-split energy-level system of the  $5f^2$  electrons of tetravalent uranium ions in  $C_{3v}$  symmetry sites in calcium fluoride. Well-delineated sharp levels, characteristic of those required by the crystal symmetry, are evident with almost complete freedom from extra lines of vibrational or other origin that have any appreciable intensity relative to the intensities of the electronic levels. The crystal-field-splittings range from two to five times greater than those for Pr<sup>3+</sup> ion in CaF<sub>2</sub> crystals, but are nevertheless in well-defined  $J$ -value groupings.

A previous study of uranium ions in calcium fluoride was made by Conway,<sup>10</sup> who showed the general aspects of the solution on a theoretical basis, but without the use of a crystal-field-splitting analysis. Work on tetravalent uranium in various crystal lattices has also been reported by McLaughlin,<sup>11</sup> Richman *et al.*,<sup>12</sup> Satten *et al.*,<sup>13, 14</sup> and others. Except for the Conway study,<sup>10</sup> in which the host crystal was calcium fluoride, these previous studies involved problems of separating vibrational transitions from pure electronic transitions. The differences in the solution presented here from previous solutions result to a considerable extent from the clarification due to the absence of strong vibrational transitions in the trigonal CaF<sub>2</sub>: U<sup>4+</sup> crystals.

The  $5f^2$  U<sup>4+</sup> ion is analogous to the  $4f^2$  Pr<sup>3+</sup> ion, which has been considerably studied in various crystal lattices. Additionally, the isolated free-ion energies of Pr<sup>3+</sup> have been experimentally determined by spectroscopic methods,<sup>15, 16</sup> and have been fitted to the standard intermediate coupling equations.<sup>15</sup> Deviations of experimental and calculated values of energy levels of these isolated free Pr<sup>3+</sup> ions amount to a maximum of about 200 cm<sup>-1</sup>, even after the introduction of a configuration-interaction correction. But even larger deviations are seen in comparing the experimental isolated free-ion levels of Pr<sup>3+</sup> with the corresponding experimentally determined levels in crystals, especially in the higher levels.

The usual method of studying energy levels of ions in crystals involves the experimental determination of the crystal-field-split levels, the identification of them by crystal symmetry properties, and then the calculation of the constants of the pertinent theoretical equations from center-of-gravity (cg) energy values of the levels of each multiplet. The values of the Slater integrals  $F_0$ ,  $F_2$ ,  $F_4$ , and  $F_6$ , of the spin-orbit interaction  $\xi$ , and of the configuration-interaction  $\alpha$ , characterize the multiplet system in a particular crystal matrix. Since some levels in the crystal are considerably different from the isolated free-ion values, factors not directly related to the free-ion energy values are dispersed by the calculations into all energies. The fitting depends upon the value of the constants chosen, but usually is the poorest where there is the strongest perturbation by intermediate coupling. For U<sup>4+</sup>, the spin-orbit coupling constant is considerably larger than for Pr<sup>3+</sup>, with a resultant stronger interplay of energies via the intermediate coupling relationships for the former ion over the latter one.

In view of the factors discussed above, a somewhat different calculation method is employed in the present report from the one commonly used. It does nothing new other than to emphasize the pure  $R$ - $S$  multiplets  $^3F_3$  and  $^3H_5$  as primary data for the determination of the solution. These multiplets are only weakly affected by the crystal field (being in the low-energy region) and are readily solved for crystal-field-split levels by high-resolution infrared spectroscopy.

The Slater integrals readily yield the following relationships, which include a Trees configuration-interaction correction,  $\alpha L(L+1)$ :

$$^3F_3 - ^3H_5 = 15F_2 + 18F_4 - 273F_6 - 18\alpha, \quad (1)$$

$$F_6 = [15F_2 + 18F_4 - (^3F_3 - ^3H_5) - 18\alpha] / 273, \quad (2)$$

$$^3P_1 = ^3H_5 + 14/3 (^3F_3 - ^3H_5) + 56\alpha, \quad (3)$$

$$\alpha = [(^3P_1 - ^3H_5) - 14/3 (^3F_3 - ^3H_5)] / 56. \quad (4)$$

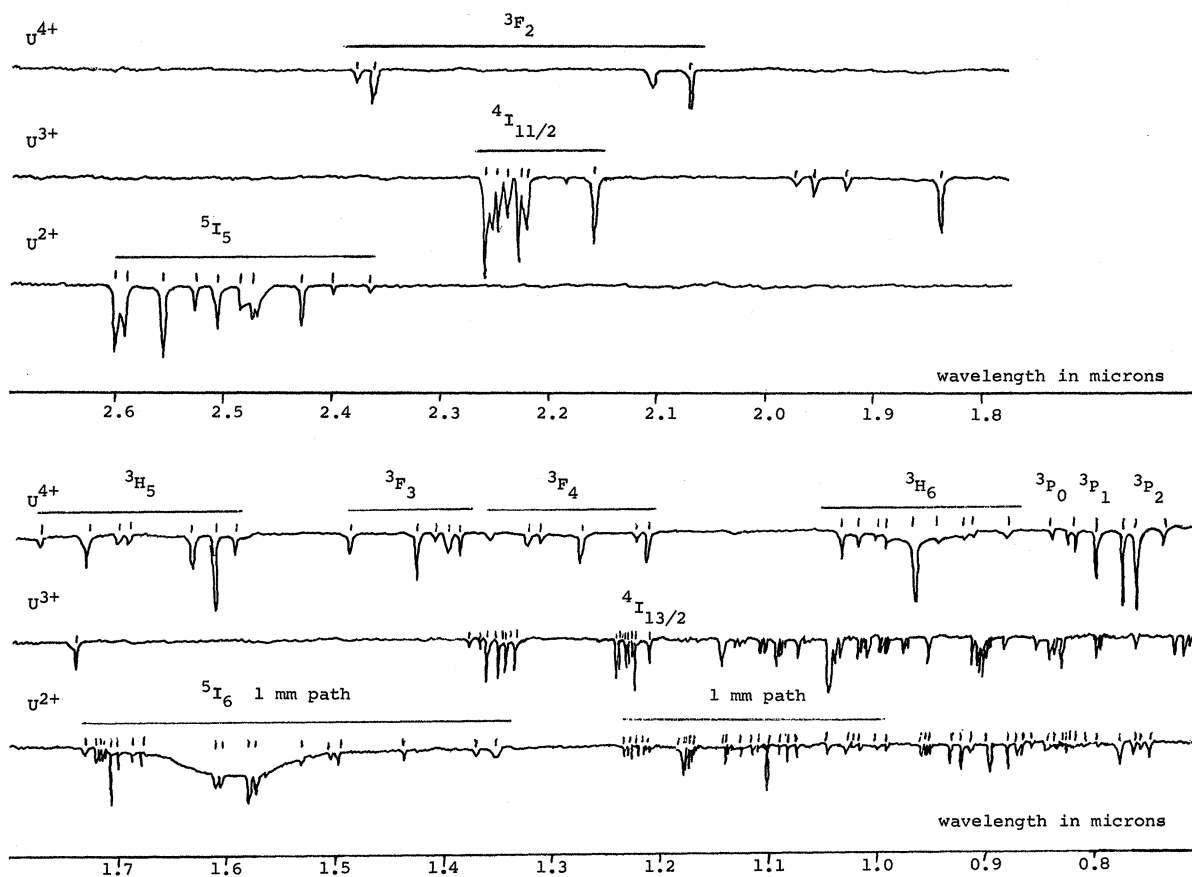
Table I contains various experimental data concerning  $f^2$  ions, and illustrates the application of Eqs. (1)–(4), to the solution for various multiplet energies. The solutions for Pr<sup>3+</sup> served as models for the CaF<sub>2</sub>: U<sup>4+</sup> calculations of the present report. Knowledge of experimental free-ion values for Pr<sup>3+</sup> allows appraisal of calculation techniques, whereas true free-ion values for U<sup>4+</sup> have not been determined.

#### Optical Spectrum of CaF<sub>2</sub>:U<sup>4+</sup>

Figure 1 summarizes the optical-absorption spectrum of trigonally sited U<sup>4+</sup> ions in calcium-

TABLE I. Free-ion energy levels for  $f^2$  ions.<sup>a</sup>

	Free ion $\text{Pr}^{3+}$ Expt <sup>b,c</sup>	Free ion $\text{Pr}^{3+}$ Calc <sup>d</sup>	Free ion $\text{Pr}^{3+}$ Calc <sup>e,f</sup>	$\text{CaF}_2:\text{Pr}^{3+}$ tetragonal Expt <sup>g</sup>	$\text{CaF}_2:\text{Pr}^{3+}$ tetragonal Calc <sup>e,h</sup>	$\text{CaF}_2:\text{U}^{4+}$ trigonal Expt <sup>i</sup>	$\text{CaF}_2:\text{U}^{4+}$ trigonal Calc <sup>e,j</sup>
${}^3H'_4$	0	147	+121	...	220	369	930
${}^3H_5$	2 152	2 214	2 152	2 256	2 256	5 980	5 980
${}^3F_3$	6 415	6 235	6 415	6 512	6 512	7 033	7 033
${}^3F_3 - {}^3H_5$	...	...	4 263	...	4 256	...	1 053
${}^3P_1$	22 008	22 018	22 046	...	22 126	12 352	12 357

<sup>a</sup>All values are cg energies in  $\text{cm}^{-1}$ .<sup>b</sup>See Ref. 15.<sup>c</sup>See Ref. 16.<sup>d</sup>See Ref. 15;  $F_0=12776$ ,  $F_2=322$ ,  $F_4=51.6$ ,  $F_6=5.14$ ,  $\zeta_f=741$ ,  $\alpha=19$ .<sup>e</sup>Calculations via Eq. (1)–(4) of present paper.<sup>f</sup> $F_0=13,617$ ,  $F_2=320$ ,  $F_4=59.2$ ,  $F_6=5.87$ ,  $\zeta_f=740$ ,  $\alpha=0$ ,  $F_6$  from Eq. (2).<sup>g</sup>W. A. Hargreaves (unpublished).<sup>h</sup> $F_0=13722$ ,  $F_2=320$ ,  $F_4=59.2$ ,  $F_6=5.89$ ,  $\zeta_f=740$ ,  $\alpha=0$ ,  $F_6$  from Eq. (2).<sup>i</sup>From present paper.<sup>j</sup> $F_0=13175$ ,  $F_2=200$ ,  $F_4=40$ ,  $F_6=8.05$ ,  $\zeta_f=1660$ ,  $\alpha=26$ ,  $F_6$  from Eq. (2).FIG. 1. Crystal-field optical-absorption spectra of  $\text{U}^{4+}$ ,  $\text{U}^{3+}$ , and  $\text{U}^{2+}$  ions in  $\text{CaF}_2$  at  $20^\circ\text{K}$ .

fluoride single crystals at 20 °K. Most of the transitions which appear in Fig. 1 are transitions from a doublet zero ground level to the crystal-field-split levels of the various multiplets. These are identified by a short vertical line adjacent to the maximum absorption position. Some other higher levels of the  ${}^3H_4$  ground multiplet have been identified experimentally by absorption measurements at temperatures higher than the 20 °K temperature involved in the data of Fig. 1. Also, identification of the upper two  ${}^3H_4$  levels was accomplished by optical emission studies at 77 °K. From a  ${}^3H_5$  level at 6226  $\text{cm}^{-1}$  there is a strong fluorescent transition to a  ${}^3H_4$  level at 652  $\text{cm}^{-1}$  (wavelength of 1.794  $\mu$ ), and a weaker transition to a  ${}^3H_4$  level at 1119  $\text{cm}^{-1}$  (wavelength of 1.958  $\mu$ ). Use is made of this optical-absorption and emission data later in the report when the crystal-field calculations and the free-ion calculations are carried out.

#### Transition Selection Rules

The nonvanishing crystal-field matrix elements in  $C_{3v}$  symmetry are grouped in Hellwege notation as  $\mu = 0$  and  $\mu = \pm 1$  with allowed values of  $q$  of 0,  $\pm 3$ , and  $\pm 6$ . For transition rule purposes,  $\mu = 0$  can be split into the irreducible representations  $A_1$  and  $A_2$ , and in similar notation the  $\mu = \pm 1$  level is an  $E$  level. Electric-dipole selection rules derived from Prather<sup>17</sup> show that the allowed transitions are  $\sigma$  for transitions between  $A_1$  or  $A_2$  and  $E$ , and  $\pi$  for transitions  $A_1$  to  $A_1$  or  $A_2$  to  $A_2$ . No transitions were seen which did not obey electric-dipole selection rules. The zero energy level of  ${}^3H_4$  is identified by experiment and calculations as an  $E$  level, allowing transitions from it to all upper levels.

#### Zeeman Studies of $\text{CaF}_2: \text{U}^{4+}$

Optical-absorption Zeeman studies were made at liquid-nitrogen and liquid-helium temperatures, with particular emphasis on the spectral region of the  ${}^3P_0$ ,  ${}^3P_1$ , and  ${}^3P_2$  levels. Absorption photographs in  $\sigma$  and  $\pi$  polarization were taken for radiation passing along the 1-cm axis path of a  $\text{CaF}_2: \text{U}^{4+}$  cylinder and dispersed by a 1.8-A/mm spectrometer, with dc magnetic field imposed along a radial [111] trigonal axis. The photographs were studied to identify degenerate levels split by the Zeeman field, and to determine the polarization of the transitions. In  $C_{3v}$  symmetry all degenerate levels should show a linear Zeeman effect for magnetic fields parallel to a trigonal axis. El'yashevich<sup>18</sup> gives a good summary of the predicted polarizations for transitions between Zeeman-split levels.

In the plates available, the  ${}^3H_4$  to  ${}^3P_0$  transition

was too weak for Zeeman analysis. In  ${}^3P_1$ , the absorption 0–12 563  $\text{cm}^{-1}$  was strongly split with the correct  $\sigma$  polarization (being an  $E$  to  $A_2$  transition); a transition 123–12 563  $\text{cm}^{-1}$  was too weak for analysis; a 0–12 247  $\text{cm}^{-1}$  ( $E$  to  $E$ ) was correctly  $\pi$ ; and a 79–12 247  $\text{cm}^{-1}$  ( $A_2$  to  $E$ ) was correctly  $\sigma$ . In  ${}^3P_2$ , the 0–13 615  $\text{cm}^{-1}$  was too weak to analyze; the 0–13 123  $\text{cm}^{-1}$  ( $E$  to  $E$ ) was correctly  $\pi$ ; and the 0–12 953  $\text{cm}^{-1}$  ( $E$  to  $A_1$ ) was correctly  $\sigma$ . Splittings were evident in other levels (e. g., in  ${}^1I_6$ ) but were not analyzed. The fact that all analyzable lines in the  ${}^3P$  manifold show predicted Zeeman characteristics is considered a favorable check on the derived solution.

Contrasting with the Zeeman spectra, no appreciable polarization of  $\text{CaF}_2: \text{U}^{4+}$  absorption spectra in zero magnetic field is observed in the infrared, visible, or ultraviolet spectral regions. This is true regardless of crystal orientation, and is apparently due to the averaging effects of the four equivalent trigonal axes.

#### Free-Ion Calculations

Table II compiles the experimental and calculated results of multiplet energies of trigonally

TABLE II. Free-ion levels of  $\text{U}^{4+}$ .

Multiplet	Expt <sup>a</sup>	Calc <sup>b</sup>	Composition <sup>c</sup>
${}^3H_4$	369	930	91% ${}^3H_4$ , 8% ${}^1G_4$ , 1% ${}^3F_4$
${}^3F_2$	4 468	3 393	92% ${}^3F_2$ , 7% ${}^1D_2$ , 1% ${}^3P_2$
${}^3H_5$	5 980	5 980	100% ${}^3H_5$
${}^3F_3$	7 033	7 033	100% ${}^3F_3$
${}^3F_4$	7 850	8 406	69% ${}^3F_4$ , 26% ${}^1G_4$ , 5% ${}^3H_4$
${}^3H_6$	10 445	10 507	94.7% ${}^3H_6$ , 5.3% ${}^1I_6$
${}^3P_0$	11 962	10 614	97.7% ${}^3P_0$ , 2.3% ${}^1S_0$
${}^3P_1$	12 357	12 357	100% ${}^3P_1$
${}^3P_2$	13 286	12 549	82% ${}^3P_2$ , 14% ${}^1D_2$ , 4% ${}^3F_2$
${}^1G_4$	14 955	15 049	66% ${}^1G_4$ , 30% ${}^3F_4$ , 4% ${}^3H_4$
${}^1I_6$	19 648	20 087	94.7% ${}^1I_6$ , 5.3% ${}^3H_6$
${}^1D_2$	23 380	21 544	78% ${}^1D_2$ , 17% ${}^3P_2$ , 5% ${}^3F_2$
${}^1S_0$		47 822	

<sup>a</sup> The cg energies in  $\text{cm}^{-1}$  based on a complete identification of crystal-field-split levels, and a subsequent weighting of singlet and doublet levels, but  ${}^1I_6$  is an average value.

<sup>b</sup> Calculated energies in  $\text{cm}^{-1}$ , with calculation based upon Eqs. (1)–(4) of this paper. The constants are  $F_0 = 13175$ ,  $F_2 = 200$ ,  $F_4 = 40$ ,  $F_6 = 8.05$ ,  $\zeta_f = 1660$ , and  $\alpha = 26$ .

<sup>c</sup> Compositions are from eigenvectors of matrix solutions.

sited  $U^{4+}$  ions in  $CaF_2$  single crystals. Calculations involve the Slater integrals and the Spedding<sup>19</sup> solutions for  $f^2$  ions in intermediate coupling. All primed multiplets represent intermediate coupling values. The configuration-interaction constant was determined from Eq. (4) of the present paper, using a cg value of  ${}^3P_1$  based on the experimentally determined crystal-field-split levels. The actual identification of the approximate energy positions of the various levels of the  ${}^3P$  multiplet was based on all aspects of the total solution, including optical absorption and Zeeman data, free-ion calculations, and crystal-field-splitting calculations.

Values of the Slater integrals  $F_0$ ,  $F_2$ , and  $F_4$  were determined by trial for a best fit to all levels. The  $F_6$  value was controlled by Eq. (2) of the paper. Since  ${}^3H_6$  is little affected by intermediate coupling,  $\zeta$  is fairly well determined by the  ${}^3H_6$  to  ${}^3H_5$  interval, and only a small amount of trial fitting was necessary to adequately determine it.

Calculations were performed on a small desk top electronic calculator, using the iterative calculation techniques of Slater,<sup>20</sup> which were adequately handled by the calculator. Final solutions involving matrices greater than  $2 \times 2$  were rechecked on a large electronic computer.

#### Crystal-Field Calculations $CaF_2:U^{4+}$

Crystal-field calculations were carried out by means of operator-equivalent methods using the tables of Low,<sup>21</sup> and also by group-theoretical methods using the Eqs. (6-3)–(6-5) of Wybourne,<sup>22</sup> the tabulated data of Nielson and Koster for  $f^2$  electrons,<sup>23</sup> and the 3- $j$ , 6- $j$  symbols of Rotenberg *et al.*<sup>24</sup> Agreement between the two methods was excellent when a comparison was made using the proportionality constants given by Weber and Bierig.<sup>25</sup> The only discrepancy indicated a required change, to the negative sign, of matrix value 55 of  $J = 6$  in Table IX of Low.<sup>21</sup>

Tables III and IV compile the crystal-field calculations into summary form, previous to the final calculation of the actual levels. The group-theoretical approach allows the direct calculation of intermediate-coupling matrix multipliers, using the wave function compositions of Table II. For example, the calculation of  ${}^1G'_4$  of  $CaF_2:U^{4+}$  involves the linear combination of wave functions:

$${}^1G'_4 = 0.814 |{}^1G_4\rangle + 0.551 |{}^3F_4\rangle - 0.186 |{}^3H_4\rangle. \quad (4)$$

The intermediate-coupling solution for  ${}^1G_4$  is as follows<sup>26</sup>:

$${}^1G'_4 = C \begin{pmatrix} Jk & J \\ Mq & M \end{pmatrix} [(0.814)^2 \langle {}^1G_4 || U^k || {}^1G_4 \rangle + (0.551)^2 \langle {}^3F_4 || U^k || {}^3F_4 \rangle + (0.186)^2 \langle {}^3H_4 || U^k || {}^3H_4 \rangle - 2(0.551)(0.186) \langle {}^3H_4 || U^k || {}^3F_4 \rangle]. \quad (5)$$

The bracketed term in Eq. 5 is a  $k$ -dependent value, which, when multiplied by  $B_q^k$ , gives the "intermediate-coupling multiplier" of Table IV, column 4.

The final calculated levels of  $CaF_2:U^{4+}$  are listed in Table V, along with the experimentally derived levels. The various  $B_q^k$  values listed in Table V are "best fit" values for matching calculated levels to experimental levels.

#### ESR $CaF_2:U^{4+}$

From Table V we see that the lowest  ${}^3H_4$  level is a doublet made up of a linear combination of the wave functions involving  $J_z$  values of  $\pm 4$ ,  $\pm 1$ , and  $\pm 2$ . Since the non-Kramers doublet is involved, spin resonance is only possible through a slight admixture, by way of symmetry distortion, of the wave function of the next higher level.

The value of  $g_{\perp}$  is zero, and  $g_{\parallel}$  can be expressed in terms of the Landé splitting factor and effective value of  $J_z$ , denoted  $J_e$  as in

$$g_{\parallel} = 2(0.8)J_e.$$

From the eigenvectors of the  ${}^3H'_4$  solution, given in Table V, the solution calculates as follows:

$$g_{\parallel} = 2. (0.8) (4a^2 + b^2 - 2c^2) = 4.80,$$

with  $a = 0.817$ ,  $b = 0.576$ , and  $c = 0.015$ .

The difference of the spectroscopically derived  $g_{\parallel}$  from the more direct spin-resonance measurement<sup>4</sup> of 4.03 lies to some extent in various approximations used in the calculation procedure. It is obvious from the discrepancies between calculated and experimental  ${}^3H'_4$  levels (for example) that a perfect calculation has not been accomplished. On the other hand, the correct  ${}^3H'_4$  doublet is in the zero-energy position, with close, but not exact, eigenfunction mixing. Also Table V shows a reasonable approximation of all calculated crystal-field-split levels to experimental values. Further refinements in energy interaction calculations might result in improved results.

#### TRIVALENT URANIUM IN CALCIUM FLUORIDE

Optical-absorption measurements of tetragonally sited  $U^{3+}$  ions in calcium fluoride at a temperature of 20°K have resulted in a modification of the energy-level scheme of the  ${}^4I$  multiplets from the presentation of the previous report.<sup>1</sup> Two new lines 4452 and 4433  $cm^{-1}$  appear in the absorption spectrum of  ${}^4I_{11/2}$  at temperatures below about 100°K. At 20°K the 4433- $cm^{-1}$  level becomes the strongest and sharpest of the group. The Kramers doublet levels of the  ${}^4I_{11/2}$  multiplet are now shown in Fig. 2 as six closely spaced levels. They do not include the two more remote lines in the 5000- $cm^{-1}$

TABLE III. Crystal-field matrix elements in trigonal symmetry.

$J$	$Q$	$K$	$J_z$	0	$\pm 1$	$\pm 2$	$\pm 3$	$\pm 4$	$\pm 5$	$\pm 6$
1	0	2		-0.3651	+0.1824					
2	0	2		-0.2389	-0.1191	+0.2389				
2	0	4		+0.2389	-0.1593	+0.0398				
				2    -1						
2	3	4		-0.2357						
3	0	2		-0.1952	-0.1464	0	+0.2440			
3	0	4		+0.1612	+0.0268	-0.1880	+0.0806			
3	0	6		-0.1825	+0.1369	-0.0547	+0.0091			
				2    -1	3    0					
3	3	4		-0.1005	-0.2132					
3	3	6		+0.1774	-0.0836					
				3    -3						
3	6	6		+0.2774						
4	0	2		-0.1699	-0.1444	-0.0679	+0.0594	+0.2378		
4	0	4		+0.1341	+0.0670	-0.0891	-0.1564	+0.1043		
4	0	6		-0.1246	+0.0062	+0.1371	-0.1059	+0.0249		
				2    -1		3    0		4    +1		
4	3	4		-0.0623		-0.1564		-0.1649		
4	3	6		+0.0903		+0.1079		-0.1365		
				3    -3		4    -2				
4	6	6		+0.1895		+0.1432				
5	0	2		-0.1527	-0.1374	-0.0916	-0.0153	+0.0961	+0.2290	
5	0	4		+0.1183	+0.0788	-0.0197	-0.1183	-0.1183	+0.1183	
5	0	6		-0.1047	-0.0314	+0.0943	+0.0759	-0.1257	+0.0393	
				2    -1	3    0	4    +1	5    2			
5	3	4		-0.0441	-0.1183	-0.1527	-0.1277			
5	3	6		+0.0608	+0.1134	+0.0175	-0.1470			
				3    -3	4    -2	5    -1				
5	6	6		+0.1592	+0.1378	+0.0824				
6	0	2		-0.1399	-0.1299	-0.0999	-0.0500	+0.0200	+0.1099	+0.2199
6	0	4		+0.1073	+0.0818	+0.0140	-0.0690	-0.1226	-0.0843	+0.1265
6	0	6		-0.0930	-0.0465	+0.0512	+0.1000	+0.0186	-0.1279	+0.0512
				2    -1	3    0	4    +1	5    2	6    3		
6	3	4		-0.0334	-0.0929	-0.1309	-0.1359	-0.1009		
6	3	6		+0.0452	+0.1000	+0.0688	-0.0408	-0.1414		
				3    -3	4    -2	5    -1	6    0			
6	6	6		+0.1414	+0.1291	+0.0957	+0.0512			

region, which were previously thought to be part of this multiplet.

Many fluorescent transitions occur at 20 °K from the  ${}^4I_{11/2}$  crystal-field-split levels to those of  ${}^4I_{9/2}$ , and these are also shown in Fig. 2. The first four fluorescent transitions are all  $\text{CaF}_2:\text{U}^{3+}$  laser transitions. The low-threshold 2.610- $\mu$  laser line is more satisfactorily explained with the new  ${}^4I_{11/2}$  level system, as originating from the lowest level of a closely spaced group. The discussion in the previous report<sup>1</sup> of the other fluorescent transitions of tetragonal  $\text{CaF}_2:\text{U}^{3+}$ , and the effect on them of a  $\text{U}^{2+}$  impurity in the crystal, is generally correct. When little or no  $\text{U}^{2+}$  contamination is present,  $\text{CaF}_2:\text{U}^{3+}$  at low temperature lases at 2.610  $\mu$ , but it lases at 2.565  $\mu$  as the crystal tem-

perature approaches room temperature. The 2.510- $\mu$   $\text{CaF}_2:\text{U}^{3+}$  has a high pumping threshold and involves considerable  $\text{U}^{3+}$  to  $\text{U}^{2+}$  energy transfer. When the  $\text{U}^{2+}$  content is very high, a ground-state  $\text{CaF}_2:\text{U}^{3+}$  laser of wavelength 2.224  $\mu$  can be made to operate at very high pumping power.

In addition to the fluorescent transitions discussed above, several others from much higher levels are reported here. A strong sharp fluorescence of wavelength 4708 Å is the result of a transition from a level at 21842  $\text{cm}^{-1}$  to the ground manifold level at 602  $\text{cm}^{-1}$ . Also a weaker fluorescence of 4685 Å is the result of a transition to 497  $\text{cm}^{-1}$  from the same upper level.

Figure 1 shows the infrared portion of the absorption spectrum of tetragonal  $\text{CaF}_2:\text{U}^{3+}$  at 20 °K.

TABLE IV. Crystal-field matrix multipliers.<sup>a</sup>

Multiplet	<i>k</i>	<i>R-S</i> Multiplier	Intermediate-coupling multiplier
<sup>3</sup> P <sub>1</sub>	2	+0.4008	
<sup>3</sup> F <sub>3</sub>	2	-0.2500	
	4	-0.0555	
	6	+0.2500	
<sup>3</sup> H <sub>5</sub>	2	+0.9587	
	4	-0.6056	
	6	-0.3485	
<sup>3</sup> F <sub>2</sub>	2	-0.2332	-0.3003
	4	-0.1177	+0.0465
<sup>3</sup> P <sub>2</sub>	2	-0.6124	-0.5309
	4	0.0000	-0.1185
<sup>1</sup> D <sub>2</sub>	2	-0.6414	-0.6515
	4	+0.7062	+0.6522
<sup>3</sup> H <sub>4</sub>	2	+0.9048	+0.8283
	4	-0.6557	-0.7305
	6	-0.6029	-0.3347
<sup>3</sup> F <sub>4</sub>	2	-0.3419	-0.1084
	4	-0.2575	-0.3953
	6	-0.1220	-0.0554
<sup>1</sup> G <sub>4</sub>	2	+0.2238	+0.0706
	4	-1.077	-0.8645
	6	+1.198	+0.9367
<sup>3</sup> H <sub>6</sub>	2	+1.109	+1.161
	4	-0.8494	-0.7318
	6	-0.8913	-0.8197
<sup>1</sup> I <sub>6</sub>	2	+2.219	+2.147
	4	+1.275	+1.155
	6	+0.3565	+0.2882

<sup>a</sup> Values to be multiplied by matrix elements of Table III and by appropriate  $B_q^k$  to determine matrix energy values in  $\text{cm}^{-1}$ .

In connection with the present study, the entire spectrum has been obtained from the longest infrared wavelengths to about 3000 Å in the ultraviolet. The mathematical analysis of these data is a considerable task, and has not been accomplished, but some interesting results are obtained from the lower (infrared) energy levels.

Since all of the <sup>4</sup>I multiplets are split in the tetragonal field into Kramers doublets, the cg values of the <sup>4</sup>I<sub>11/2</sub> and <sup>4</sup>I<sub>9/2</sub> can be readily determined as 4500 and 313  $\text{cm}^{-1}$ , respectively. If *L-S* coupling is approximately true for these low levels, the  $\zeta_{5f}$  value for U<sup>3+</sup> computes to be 1520. From this value of  $\zeta_{5f}$ , an *L-S* coupling position for <sup>4</sup>I<sub>13/2</sub> is calculated at 9433  $\text{cm}^{-1}$ , and similarly for <sup>4</sup>I<sub>15/2</sub> at 15133  $\text{cm}^{-1}$ . Inspection of Fig. 1 shows that above the <sup>4</sup>I<sub>11/2</sub> absorption levels at 4500  $\text{cm}^{-1}$  there are some weak lines in the 5100- $\text{cm}^{-1}$  (1.96- $\mu$ ) region, and two strong sharp lines at 5446  $\text{cm}^{-1}$  (1.836  $\mu$ ) and 5747 (1.740  $\mu$ ). These groups do not appear to be connected to the <sup>4</sup>I<sub>13/2</sub> multiplet, which in tetragonal symmetry would consist of seven crystal-

field-split lines. A group of eight lines at 7410- $\text{cm}^{-1}$  cg (1.35- $\mu$  region), or a group of seven lines at 8154- $\text{cm}^{-1}$  cg (1.23- $\mu$  region), are more likely candidates for <sup>4</sup>I<sub>13/2</sub>.

The lines between <sup>4</sup>I<sub>11/2</sub> and <sup>4</sup>I<sub>13/2</sub>, mentioned above, would then be penetrations of the energy region occupied mainly by the <sup>4</sup>I multiplets by other multiplets. This is suggested by the energy-level scheme of Fig. 21 of Dieke,<sup>27</sup> which is a survey-type analysis based upon intermediate-coupling calculations for a hydrogenic atom, with estimated field constants. The several weak lines sitting on top of a high transmission band of CaF<sub>2</sub>: U<sup>3+</sup> near 5100  $\text{cm}^{-1}$  are about 600  $\text{cm}^{-1}$  from the very strong <sup>4</sup>I<sub>11/2</sub> levels and may be vibrational in origin.

#### DIVALENT URANIUM IONS IN CALCIUM FLUORIDE

Evidence showing the existence of divalent uranium ions in calcium-fluoride single crystals was presented in the previous report.<sup>1</sup> The evidence involved studies of the ion as it exists in the unusual physical environment of an impurity site in a crystal. The U<sup>2+</sup> ion in the CaF<sub>2</sub> crystal is in a stable and permanent condition even at room temperature. However, any attempts to remove it from the crystal to study chemical or other properties would be unsuccessful, since conversion to U<sup>3+</sup> or U<sup>4+</sup> ions would be almost spontaneous.

An interesting and rather convincing experiment can be added to the evidence of the previous report to substantiate the U<sup>2+</sup> ion identification. The green crystals of CaF<sub>2</sub>: U<sup>2+</sup> can be heated for 2 h in high vacuum, in contact only with platinum, at a temperature of 1100 °C, and partially converted to CaF<sub>2</sub>: U<sup>3+</sup>. The evidence of conversion is an optical-absorption study showing a substantial decrease, following the heat treatment, of the characteristic U<sup>2+</sup> absorption levels in the 2.5- $\mu$  region, and the appearance of definitive U<sup>3+</sup> 2.15- and 2.22- $\mu$  strong absorption lines.

In conjunction with ESR studies which show the ion in question (U<sup>2+</sup>) to be of even valence, further optical studies also confirm the identification.

The U<sup>4+</sup> ion is 5f<sup>2</sup> and would have 13 possible free-ion energy levels. In a crystal of C<sub>3v</sub> symmetry, these free-ion levels would be split into 61 levels, and in lowest crystal symmetry would completely split into 91 nondegenerate levels.

A study of the optical-absorption levels of CaF<sub>2</sub>: U<sup>2+</sup> at 20 °K has been made, and 162 sharp absorption transitions from the ground-zero level are evident in the wavelength region from 8  $\mu$  in the infrared to 3000 Å in the ultraviolet. There is reason to assume more absorption levels to exist further down in the ultraviolet. The transitions appear in characteristic crystal-field-split groupings, as can be seen in the infrared portion of the spectrum

TABLE V. Crystal-field-splitting levels<sup>a</sup> of trigonally sited  $U^{4+}$  ions in Calcium-Fluoride single crystal at 20 °K. Crystal-field constants are  $B_0^2 = -1440$ ,  $B_0^4 = +1000$ ,  $B_0^6 = -1000$ ,  $B_2^4 = \pm 4000$ ,  $B_2^6 = \pm 4130$ , and  $B_4^6 = \pm 1085$ .

Multiplet	Expt energy and degeneracy						Calc energy and degeneracy							
${}^3H_4$	0	79	103	123	652	1119	0	461	765	1002	1331	1436		
	<i>E</i>	$A_2$	$A_1$				$E^b$	$A_2$	$A_1$	<i>E</i>	$A_1$	<i>E</i>		
${}^3F_2$	0	18	620				0	27	207					
	4216	4234	4836				$A_1$	<i>E</i>	<i>E</i>					
${}^3H_5$	0	141	241	276	481	568	637	0	63	364	460	578	720	794
	5660	5800	5898	5935	6140	6227	6296	<i>E</i>	<i>E</i>	<i>A</i>	<i>A</i>	<i>E</i>	<i>A</i>	<i>E</i>
${}^3F_3$	0	289	379	435	493			0	109	250	410	424		
	6743	7032	7122	7178	7236			<i>E</i>	<i>A</i>	<i>A</i>	<i>A</i>	<i>E</i>		
${}^3F_4$	0	196	266	495	822	893		0	4	352	383	610	648	
	7385	7581	7651	7880	8207	8278		<i>A</i>	<i>E</i>	<i>E</i>	<i>A</i>	<i>E</i>	<i>A</i>	
${}^3H_6$	0	154	322	511	672	921		0	68	365	939	1068	1217	
	1173	1305	1720					1562	1630	1806				
	9708	9862	10030	10219	10380	10629		<i>A</i>	<i>A</i>	<i>E</i>	<i>E</i>	<i>A</i>	<i>E</i>	
	10881	11013	11428					<i>E</i>	<i>A</i>	<i>A</i>				
${}^3P_0$	11962	$A_1$						11962	$A_1$					
${}^3P_1$	0		316					0	316					
	11247	<i>E</i>	12563	$A_2$				<i>E</i>	$A_2$					
${}^3P_2$	0		170		662			0	230	532				
	12953	$A_1$	13123	<i>E</i>	13615	<i>E</i>		$A_1$	<i>E</i>	<i>E</i>				
${}^1G_4$	0	240	487	652	1080	1759		0	116	1081	1302	2481	2854	
	14267	14507	14754	14919	15347	16026		<i>E</i>	<i>A</i>	<i>E</i>	<i>A</i>	<i>E</i>	<i>A</i>	
${}^1D_2$	0	976	1104					0	571	1312				
	22548	23524	23652					<i>E</i>	$A_1$	<i>E</i>				

<sup>a</sup> Energy levels in  $cm^{-1}$ .

<sup>b</sup> One of the states of the lowest  ${}^3H_4$  doublet is  $0.817|4\rangle - 0.576|1\rangle - 0.015|-2\rangle$ .

shown in Fig. 1. Such an absorption spectrum of an even-valence ion is only explainable if the ion is  $U^{2+}$  of configuration  $5f^4$ ,  $5f^3d$ , or  $5f^3s$ .

The  $CaF_2: U^{2+}$  was previously assumed<sup>1</sup> as  $5f^3d$ , with ground state  ${}^5L_6$ , but evidence now indicates  $5f^3s$  as the true configuration. Figure 3 shows the lowest levels of  $CaF_2: U^{2+}$ , based on absorption and fluorescence measurements. The approximate average energies of the two lowest multiplets are  $4000\text{ cm}^{-1}$  for  ${}^5I_5$  and  $100\text{ cm}^{-1}$  for  ${}^5I_4$ . Assuming  $L$ - $S$  coupling as a rough approximation, we calculate  $\zeta_{5f}$  as  $2(3900/5)$  or  $1560$ . From Judd,<sup>28</sup> we have the relationships

$$\zeta_U^{1+} \approx \zeta_U^{2+} \approx \zeta_U^{3+}.$$

The  $\zeta_{5f}$  value calculated for  $U^{3+}$  in the present report is  $1520$ , about the same as that for  $U^{2+}$ . A similar calculation using  ${}^5L_6$  and  ${}^5L_7$  as the  $CaF_2: U^{2+}$  multiplets shows unsatisfactory agreement.

The  $5f^3d$  configuration would have  $386$  free-ion levels which would split in a crystal of low symmetry to  $3640$  nondegenerate levels. For a higher

symmetry there would be considerably less than  $3640$  levels, but still a large number. The configuration  $5f^3s$  has  $82$  free-ion levels, and  $728$  levels in a crystal of lowest symmetry. This appears a more likely relationship to the observed  $162$  crystal-field-split lines found in the covered portion of the optical-absorption spectrum of  $CaF_2: U^{2+}$ .

In trigonal symmetry the  ${}^5I_4$  level would show  $6$  crystal-field split lines with  $7$  lines for  ${}^5I_5$  and  $9$  lines for  ${}^5I_6$ . Table VI lists the levels of  $CaF_2: U^{2+}$  in the infrared region as determined from absorption measurements. If these are various  ${}^7I$  multiplet groupings, it is evident that the multiplets exhibit more crystal-field-split lines than called for in trigonal symmetry. A tentative explanation of this is also a tentative explanation for the existence of  $U^{2+}$  ions in noncubic sites in  $CaF_2$ . Precision density measurements indicate that  $U^{2+}$  ions in the  $CaF_2$  lattice are in *addition* sites, discussed in the previous report.<sup>1</sup> The density of a  $CaF_2: U^{2+}$  crystal with a measured  $U^{2+}$  content is too high to be explained on a substitutional basis. As in the

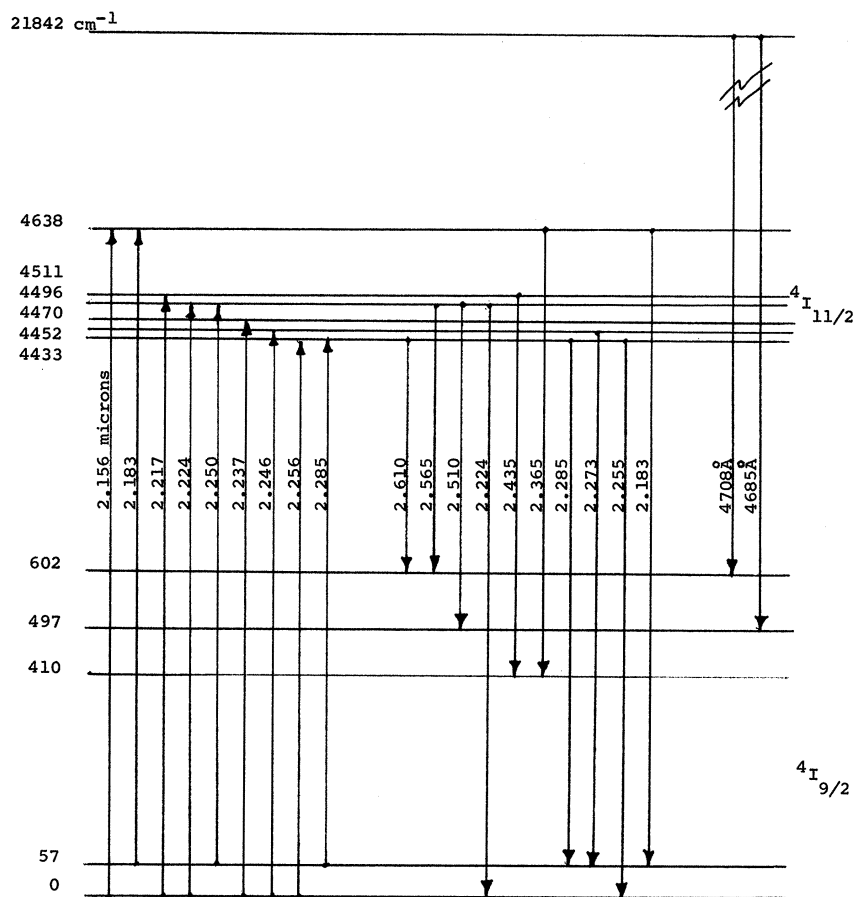


FIG. 2. Optical absorption and fluorescence transitions involving the lower energy levels of tetragonal  $U^{3+}$  ions in calcium fluoride at 20 °K. The energy scale breaks between free-ion states.

prebros report, it is postulated that  $U^{2+}$  ions enter normally vacant interstitial sites with two  $F^-$  compensating ions in two nearest, normally empty, interstitial sites having a contiguous edge. The resultant charge compensation is not in a [111] crystal direction as in  $CaF_2:U^{4+}$ , but [112]. This [112] compensation direction would yield lower symmetry than  $C_{3v}$ , with a resultant increase in the number of crystal-field-split lines for a given multiplet. In a (110) plane, the ESR spectrum of a [112] site would appear very much like a [111] site spectrum. The corresponding angles between site axes are complementary in the two cases, and the spectrum of the [111] compensation sites would be shifted 90° (with respect to an [001] crystal direction) from the spectrum of [112] compensation sites.

Much remains to be done in the analysis of  $CaF_2:U^{2+}$  but all of the evidence available seems to show that it is been properly identified, and to some extent characterized by some definite physical properties.

#### TEMPERATURE SHIFT OF URANIUM-ION ENERGY LEVELS

During the course of the work on energy levels of uranium ions in calcium fluoride it was found that some energy-level positions were affected by crystal temperatures. The effect is of interest in itself, but is also of importance in establishing definitive wavelength and energy values for the levels. Johnson *et al.*<sup>29</sup> have reported on the thermal shifting of  $Nd^{3+}$  levels in  $LaF_3$ , and they refer to other reports concerning this effect.

Figure 4 shows the thermal shifting of all levels of the  $^3H_5$  multiplet of  $CaF_2:U^{4+}$  towards lower energies with increasing temperature. Similar results were found for other multiplets of  $U^{4+}$ , with magnitudes of shift up to two times those occurring in  $^3H_5$ .

Careful measurements on tetragonal  $CaF_2:U^{3+}$  showed no evidence of a shift in any of the infrared energy levels within a temperature range from 20

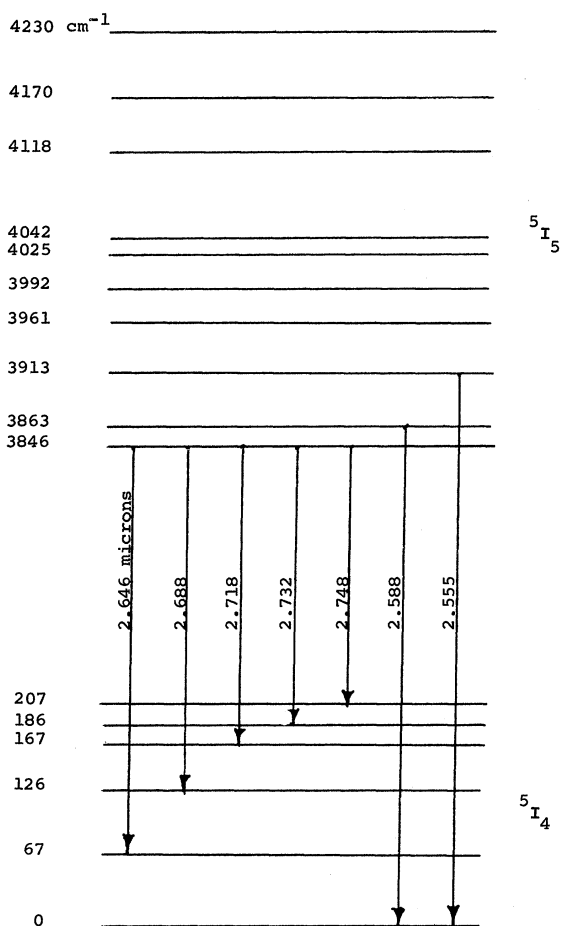


FIG. 3. Optical absorption and fluorescence transitions involving the lower energy levels of  $U^{2+}$  ions in calcium fluoride at 20°K. The energy scale breaks between free-ion states.

to 180°K. Any energy shift exceeding  $0.5 \text{ cm}^{-1}$  would be readily detected in the measurement procedure used.

Contrary to  $CaF_2:U^{4+}$ , all infrared energy levels of  $CaF_2:U^{2+}$  of sufficient sharpness for analysis were found to shift to higher energies with increasing temperature. This is shown in Fig. 4 for the  $^5I_5$  multiplet of  $U^{2+}$ . Many other levels in the 1.1- and 1.6- $\mu$  regions showed the same order of temperature shift.

#### DISCUSSION

The identification of  $U^{2+}$  ions in crystals is the most controversial subject covered by the author. Spin-resonance results, particular experiments, or calculations are not individually conclusive on this question. The present paper covering analyses of crystal-field spectra supplements the physical and chemical studies of the earlier paper. All of the evidence, when analyzed as a whole, leaves little room for question of the correctness of the identification of the various uranium ions.

#### ACKNOWLEDGMENTS

The use of magnet facilities at the MIT National Magnet Laboratory, and the cooperation of Dr. R. Sarup and Dr. F. Kaseta, College of the Holy Cross, in obtaining the Zeeman spectrographs is gratefully acknowledged.

TABLE VI. Infrared energy levels in  $\text{cm}^{-1}$  of  $CaF_2:U^{2+}$  at 20°K.

Seven lines of low oscillator strength, with average energy $10\,669 \text{ cm}^{-1}$ :									
11 132	10 965	10 869	10 730	10 504	10 373	10 330			
Seventeen lines of high oscillator strength, with average energy $9\,075 \text{ cm}^{-1}$ :									
10 070	9 842	9 718	9 569	9 320	9 251	9 200	9 099	9 009	
8 952	8 889	8 780	8 606	8 540	8 511	8 482	8 439		
Seven lines of very low oscillator strength, with average energy $8\,104 \text{ cm}^{-1}$ :									
8 347	8 230	8 210	8 150	8 117	7 936	7 740			
Eighteen lines of very high oscillator strength, with average energy $6\,315 \text{ cm}^{-1}$ :									
7 418	7 315	6 969	6 707	6 653	6 540	6 365	6 333	6 242	
6 215	5 970	5 935	5 886	5 865	5 834	5 827	5 817	5 784	
Ten lines of low oscillator strength, with average energy $4\,016 \text{ cm}^{-1}$ :									
4 230	4 170	4 118	4 042	4 025	3 992	3 961	3 913	3 863	3 846
Six lines with average energy $125 \text{ cm}^{-1}$ :									
207	186	167	126	67	0				

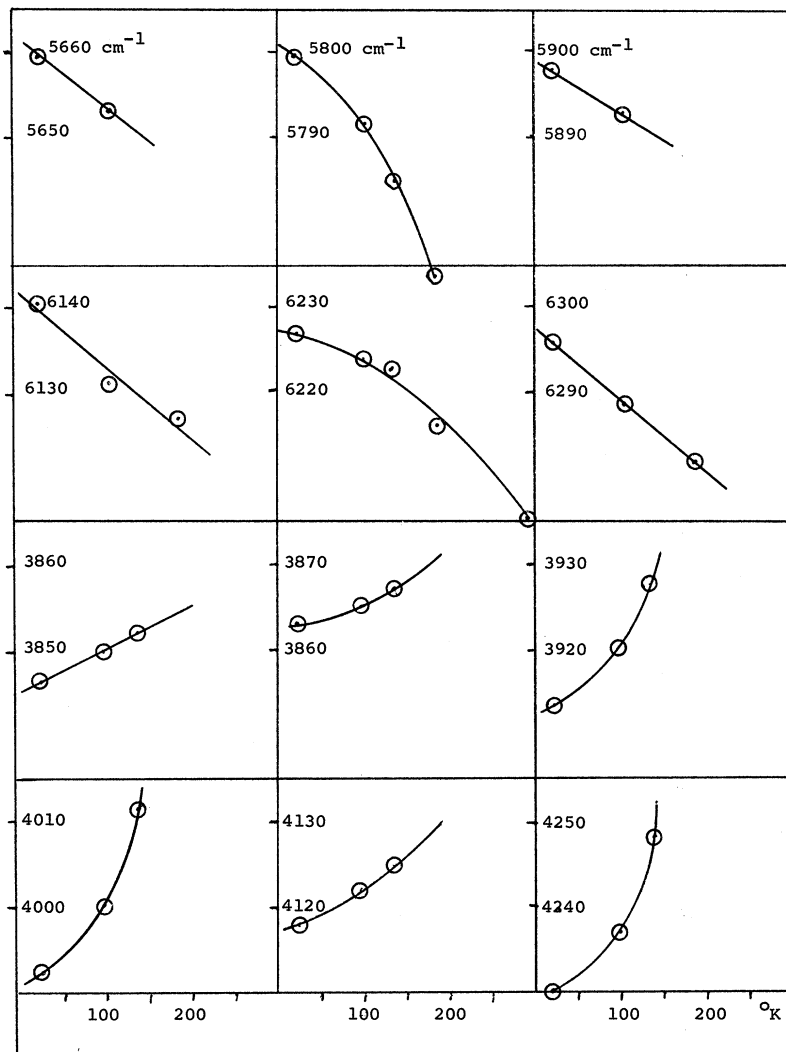


FIG. 4. Temperature shifts of crystal-field-split energy levels in the  ${}^3H_5$  multiplet of  $\text{CaF}_2:\text{U}^{4+}$  (upper six curves), and similarly for the  ${}^5I_5$  multiplet of  $\text{CaF}_2:\text{U}^{2+}$  (lower six curves). Ordinates of curves are energies of levels in  $\text{cm}^{-1}$ , and abscissas are temperatures in  $^\circ\text{K}$ .

- <sup>1</sup>W. A. Hargreaves, *Phys. Rev.* **156**, 331 (1967).  
<sup>2</sup>P. F. McDonald, E. L. Wilkinson, and R. A. Jensen, *J. Phys. Chem. Solids* **28**, 1629 (1967).  
<sup>3</sup>B. Bleaney, P. M. Llewellyn, and D. A. Jones, *Proc. Phys. Soc. (London)* **B69**, 858 (1956).  
<sup>4</sup>H. C. Meyer, P. F. McDonald, and J. D. Stettler, *Phys. Letters* **24A**, 569 (1967).  
<sup>5</sup>S. D. McLaughlan, *Phys. Rev.* **150**, 118 (1966).  
<sup>6</sup>G. C. Wetsel, Jr., *J. Appl. Phys.* **39**, 692 (1968).  
<sup>7</sup>McPherson model 218, 0.3 m, 0.6A resolution; manufactured by McPherson Instrument Corporation, Acton, Mass.  
<sup>8</sup>Model 131, manufactured by Brower Laboratories, 237 Riverview Avenue, Newton, Mass.  
<sup>9</sup>Model AC-2-110, manufactured by Air Products and Chemicals, Inc., Allentown, Pa.  
<sup>10</sup>J. G. Conway, *J. Chem. Phys.* **31**, 1002 (1959).  
<sup>11</sup>R. McLaughlin, *J. Chem. Phys.* **36**, 2699 (1962).  
<sup>12</sup>I. Richman, P. Kisliuk, and E. Y. Wong, *Phys. Rev.* **155**, 262 (1967).  
<sup>13</sup>R. A. Satten, D. Young, and D. M. Gruen, *J. Chem. Phys.* **33**, 1140 (1960).  
<sup>14</sup>R. A. Satten, C. L. Schreiber, and E. Y. Wong, *J. Chem. Phys.* **42**, 162 (1965).  
<sup>15</sup>J. Sugar, *J. Opt. Soc. Am.* **55**, 1058 (1965).  
<sup>16</sup>H. M. Crosswhite, G. H. Dieke, and W. J. Carter, *J. Chem. Phys.* **43**, 2047 (1965).  
<sup>17</sup>J. L. Prather, *Natl. Bur. Std. (U. S.) Monograph No. 19 (19xx)*, Table 13.  
<sup>18</sup>M. A. El'yashevich, U. S. Atomic Energy Commission Report No. USAEC-tr-4403, Book 1, p. 292.  
<sup>19</sup>F. H. Spedding, *Phys. Rev.* **58**, 255 (1940).  
<sup>20</sup>J. C. Slater, *Quantum Theory of Atomic Structure* (McGraw-Hill, New York, 1960), Vol. 1.  
<sup>21</sup>W. Low, *Solid State Physics*, Supplement 2 (Academic, New York, 1960).  
<sup>22</sup>B. G. Wybourne, *Spectroscopic Properties of Rare Earths* (Interscience, New York, 1965).  
<sup>23</sup>C. W. Nielson and G. F. Koster, *Spectroscopic Coefficient for the p<sup>n</sup>, d<sup>n</sup>, and f<sup>n</sup> Configurations* (The MIT Press, Cambridge, Mass., 1963).  
<sup>24</sup>M. Rotenberg, R. Bivins, N. Metropolis, and J. K.

Wooten, Jr., *The 3-j and 6-j Symbols* (MIT Technology Press, Cambridge, Mass., 1959).

<sup>25</sup>M. J. Weber and R. W. Bierig, *Phys. Rev.* **134A**, 1492 (1964), Table IV.

<sup>26</sup>J. B. Gruber and J. G. Conway, *J. Chem. Phys.* **32**, 1531 (1960).

<sup>27</sup>G. H. Dieke, *Spectra and Energy Levels of Rare Earth Ions In Crystals* (Interscience, New York, 1968).

<sup>28</sup>B. R. Judd, *Phys. Rev.* **125**, 613 (1962).

<sup>29</sup>S. A. Johnson, H. G. Freies, A. F. Schawlow, and W. M. Yen, *J. Opt. Soc. Am.* **57**, 734 (1967).

PHYSICAL REVIEW B

VOLUME 2, NUMBER 7

1 OCTOBER 1970

## Nuclear Magnetic Resonance in the Cesium-Graphite Intercalation Compounds\*

G. P. Carver†

*Laboratory of Atomic and Solid State Physics, Cornell University, Ithaca, New York 14850*

(Received 20 April 1970)

The  $C^{13}$  and  $Cs^{133}$  nuclear magnetic resonances have been studied in powdered samples of the cesium-graphite intercalation compounds at temperatures between 1.3 and 4.2°K. The spin-lattice relaxation times and the line shapes of both nuclear species in the compounds and of the  $C^{13}$  nucleus in pure graphite were measured in an effort to determine the nature of the conduction-electron states in these substances. At 4.2°K, using pulse techniques, the measured values of  $T_1$  for  $C^{13}$  are  $1.6 \pm 0.3$ ,  $2.6 \pm 0.4$ ,  $3.9 \pm 0.5$ ,  $5.6 \pm 0.5$ ,  $7.6 \pm 0.8$ , and  $30 \pm 5$  min in  $C_8Cs$ ,  $C_{24}Cs$ ,  $C_{36}Cs$ ,  $C_{48}Cs$ ,  $C_{60}Cs$ , and pure graphite, respectively. Both the Salzano-Aronson binding model for the compounds and a tight-binding extension to the Slonczewski-Weiss band model for graphite are shown to account qualitatively for the cesium concentration dependence of the  $C^{13}$   $T_1$ 's. None of the usual relaxation mechanisms is conclusively identified with the relatively short  $C^{13}$   $T_1$ 's. The temperature dependence also remains unaccounted for. Echo techniques at helium temperatures establish the shape of the 500-G-wide cesium quadrupolar spectrum in  $C_8Cs$  at 1.3°K. The measured quadrupolar splitting is  $16.8 \pm 1$  kHz. The Knight shift for cesium in  $C_8Cs$  is measured to be  $(0.29 \pm 0.01\%)$ , independent of temperature from 300 to 1.3°K. In  $C_{24}Cs$  and  $C_{36}Cs$ , the Knight shift was zero within  $\pm 0.02\%$ . The experimentally measured  $T_1$  for  $Cs^{133}$  in  $C_8Cs$  was  $7.5 \pm 0.5$  sec, while the  $T_1$ 's in  $C_{24}Cs$  and  $C_{36}Cs$  were  $27 \pm 6$  and  $48 \pm 10$  min, respectively. The  $Cs^{133}$  Knight-shift and relaxation-time results support the view that the cesium is partially ionized in  $C_8Cs$  and completely ionized in the cesium-poorer stages.

### I. INTRODUCTION

The techniques of nuclear magnetic resonance (NMR) have provided detailed information about interactions between nuclei and their environments in a variety of physical systems. This paper reports on the use of these techniques to study one member of an unusual group of crystalline, metal-like compounds, the alkali-graphite intercalation compounds.

The crystal structure of these compounds is well known.<sup>1-3</sup> Their static susceptibilities have been measured and are paramagnetic, in contrast to the large diamagnetism of pure graphite.<sup>4</sup> Electrical conductivity in the potassium-graphite system increases with increasing alkali concentration, although with different rates in the two different crystal directions.<sup>5</sup> Thermodynamic properties, such as energies of formation and alkali vapor pressures, have been measured.<sup>6</sup> The most alkali-rich stages of the cesium, rubidium, and potassium compounds have been observed to undergo a superconducting transition.<sup>7</sup> The critical field is anisotropic. More recently, an expansion of the carbon-carbon bond length with increasing alkali content

has been observed in the potassium-graphite system.<sup>8</sup>

In general, experimental results are consistent with the assumption that there is a transfer of electronic charge from alkali to the graphite layers. However, little detailed information about the nature of the resulting electronic states is available. The electrostatic binding model of Salzano and Aronson<sup>9,10</sup> successfully accounts for the bonding energies of all but the two most alkali-rich stages. However this model is not sensitive to the nature of the electronic states.

We report here on the low-temperature magnetic resonance properties of graphite and the cesium-graphite system. The only previous observation of magnetic resonance in these compounds is the work of Jensen, O'Reilly, and Tsang.<sup>11</sup> They observed the cw peak of the  $Cs^{133}$  line in  $C_8Cs$  and  $C_{24}Cs$  — a "line" that in this study is shown to be the central peak of a quadrupolar broadened powder pattern. Their quoted values for the cesium Knight shift are in disagreement with results presented here.

Section II is devoted to a brief discussion of the